NANOPOROUS MOF OF $[HgX_4]^{2-}$ $[R]^{2+}$ WITH STRUCTURAL AND OPTO-ELECTRICAL APPLICATIONS

Dinesh Jasrotia*, Bikram Singh*, Ajit Kumar**, Mukesh Kumar*, Sanjay K. Verma* & P. A. Alvi**

* GGM Science College, Cluster University of Jammu, Jammu & Kashmir
** Department of Physics and Material Science, Banasthali University, Newai, Rajasthan

Abstract:
Discoveries of novel functional materials have played very important roles to the development of science and technologies and among the diverse materials, metal-organic framework (MOF) are rapidly emerging as a unique type of porous and organic/inorganic hybrid materials which can be simply self-assembled from their corresponding inorganic metal ions/clusters with organic linkers and can be straightforwardly characterized by various analytical methods. In terms of porosity, they are superior to other well-known porous materials; exhibiting extremely high porosity with surface area upto 7000 m^2/g tunable pore size and metrics through the interplay of both organic and inorganic components with the pore sizes ranging from 3 to 100 Å and lowest framework density down to $0.13 g/cm^3$. The crystals of the $[HgCl_4]^-$ $[C_5H_6 \ N_2Cl]^+$, a MoF has been achieved by solution growth through slow cooling technique. The hybrid derivative exists in the $P2_1/c$ symmetry and is stabilized by holding the inorganic component (tetrachloromercurate) with the organic moiety through hydrogen bonding interactions. Which predict that such materials have potential electro-optical properties.
Key Words: MOF Growth, Electro-Optical Properties, Structural Parameters & XRD, FESEM.

1. Introduction:

Discoveries of novel functional materials have played very important roles to the development of science and technologies and thus to benefit our daily life. Among the diverse materials, metal–organic framework (MOF) materials are rapidly emerging as a unique type of porous and organic/inorganic hybrid materials which can be simply self-assembled from their corresponding inorganic metal ions/clusters with organic linkers, and can be straightforwardly characterized by various analytical methods [1]. In terms of porosity, they are superior to other well-known porous materials such as zeolites and carbon materials; exhibiting extremely high porosity with surface area up to 7000 m^2/g, tunable pore sizes, and metrics through the interplay of both organic and inorganic components with the pore sizes ranging from 3 to 100 Å, and lowest framework density down to 0.13 g/cm^3 [2]. Such unique features have enabled metal–organic frameworks to exhibit great potentials for a broad range of applications in gas storage, gas separations, enantioselective separations, heterogeneous catalysis, chemical sensing and drug delivery [3]. On the other hand, metal–organic frameworks can be also considered as organic/inorganic self-assembled hybrid materials, we can take advantages of the physical and chemical properties of both organic and inorganic components to develop their functional optical, photonic, and magnetic materials. Furthermore, the pores within MOFs can also be utilized to encapsulate a large number of different species of diverse functions, so a variety of functional MOF/composite materials can be readily synthesized [1].

In this Account, we describe our recent research progress on pore and function engineering to develop functional MOF materials. We have been able to tune and optimize pore spaces, immobilize specific functional groups, and introduce chiral pore environments to target MOF materials for methane storage, light hydrocarbon separations, enantioselective recognitions, carbon dioxide capture, and separations. The intrinsic optical and photonic properties of metal ions and organic ligands, and guest molecules and/or ions can be collaboratively assembled and/or encapsulated into their frameworks, so we have realized a series of novel MOF materials as ratiometric luminescent thermometers, O_2 sensors, white-light-emitting materials, nonlinear optical materials, two-photon pumped lasing materials, and two-photon responsive materials for 3D patterning and data storage [4].

Thanks to the interplay of the dual functionalities of metal–organic frameworks (the inherent porosity, and the intrinsic physical and chemical properties of inorganic and organic building blocks and encapsulated guest species), our research efforts have led to the development of functional MOF materials beyond our initial imaginations [5]. Metal–organic frameworks (MOFs) are a class of hybrid materials with unique optical and electronic properties arising from rational self-assembly of the organic linkers and metal ions/clusters, yielding myriads of possible structural motifs [6]. The combination of order and chemical tunability, coupled with good environmental stability of MOFs, are prompting many research groups to explore the possibility of incorporating these materials as active components in devices such as solar cells, photodetectors, radiation detectors, and chemical sensors. Although

International Journal of Current Research and Modern Education (IJCRME)
Impact Factor: 6.725, ISSN (Online): 2455 - 5428
(www.rdmodernresearch.com) Volume 2, Issue 2, 2017

this field is only in its incipiency, many new fundamental insights relevant to integrating MOFs with such devices have already been gained [7]. We focus our attention on the basic requirements and structural elements needed to fabricate MOF-based devices and summarize the current state of MOF research in the area of electronic, opto-electronic and sensor devices [8]. We summarize various approaches to designing active MOFs, creation of hybrid material systems combining MOFs with other materials, and assembly and integration of MOFs with device hardware. Critical directions of future research are identified, with emphasis on achieving the desired MOF functionality in a device and establishing the structure–property relationships to identify and rationalize the factors that impact device performance.

2. Experimental:

All chemicals were purchased from Sigma-Aldrich without further purification. Growth of single crystal $[HgCl_4]^-$ $[C_5H_6 N_2Cl]^+$ nanowire arrays were grown on FTO substrate using a hydrothermal based method, 0.83 mL of $[C_5H_6 N_2Cl]^+$ was mixed with 50 mL of 6 M hydrochloric acid and stirred for 5 min. Afterwards, the growth solution was transferred into a 100 mL Teflon-lined stainless steel autoclave, followed by placing a few pieces of pre-cleaned FTO glass. The hydrothermal reaction was conducted in an electronic oven at 150 °C for 5 h. After reaction, the $[HgCl_4]^-$ $[C_5H_6 N_2Cl]^+$ covered FTO glass was taken out, rinsed thoroughly with deionized water and dried with flowing nitrogen. To improve the crystallinity and conductivity of $[HgCl_4]^-$ $[C_5H_6 N_2Cl]^+$ nanowire arrays, further annealing was performed in air at 450 °C for 30 min. X-ray diffraction (XRD) patterns were collected on a Bruker AXS D8 Advance diffractometer using nickel-filtered Cu Kα radiation ($\lambda = 1.5406$ Å). Field emission scanning electron microscope (FESEM) images were taken on a JEOL JSM-7600 with an accelerating voltage of 5 kV. Transmission electron microscopy (TEM) images were taken on a JEOL JEM 2010F at an accelerating voltage of 200 kV. UV–visible spectra were recorded using a Perkin-Elmer Lambda 900 UV–vis–NIR spectrometer equipped with an integrating sphere.

3. Results and Discussion:

The XRD peak profile pattern of bis[2-amino-5-chloropyridine tetrachloromercurate(II) hybrid material has been presented in Figure 1 depicts the crystalline nature of the material with highest peak of 9406 counts per seconds for (0 3 2) hkl reflection at 2θ = 10.91° and the minimum peak of 520 for (0 3 3) hkl at 2θ = 13.91°.

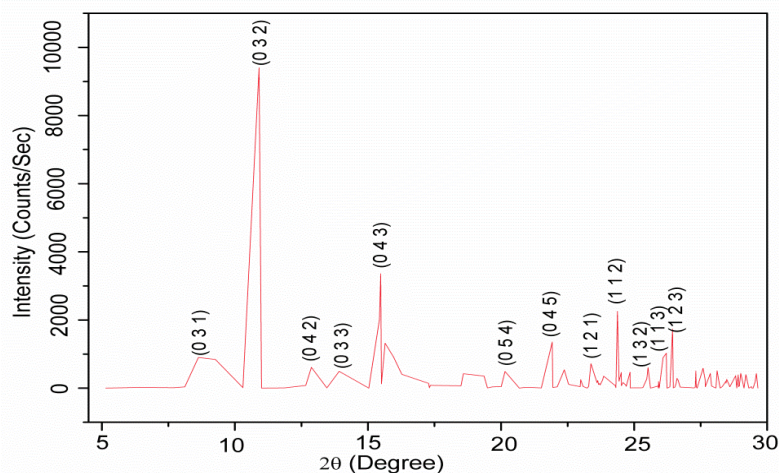Figure 1: XRD Peak profile of $[HgCl_4]^-$ $[C_5H_6 N_2Cl]^+$ MOF.
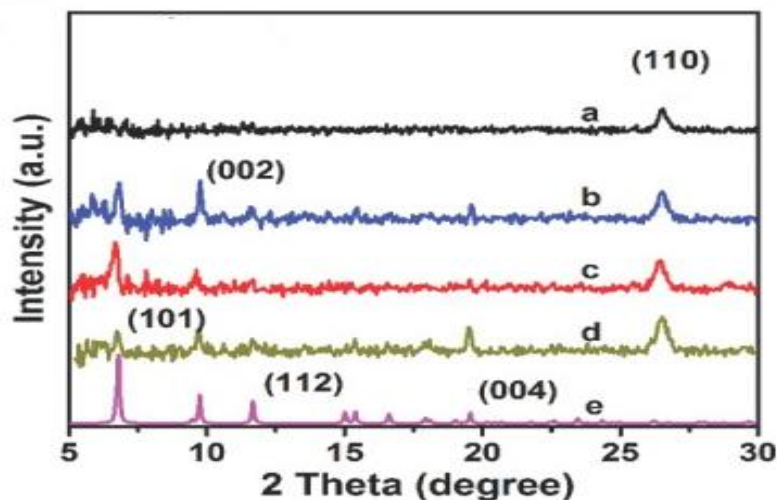
Figure 2: XRD patterns of MOF's nanocomposites

International Journal of Current Research and Modern Education (IJCRME)
Impact Factor: 6.725, ISSN (Online): 2455 - 5428
(www.rdmodernresearch.com) Volume 2, Issue 2, 2017

The XRD peak pattern was analyzed by Winplot 3D function [9] and the structure profile refinement of the XRD data was done by FullProf software [10] which results that the hybrid material exist in monoclinic space group $P2_1/c$ with lattice parameters; a = 3.894(2)Å, b = 33.347(2)Å, c = 22.130(2)Å, α = 90°, β = 95.76°, γ = 90°; unit cell volume = 3247.0(3)Å^3, crystallite size = 42.6nm. The XRD pattern of the inorganic-organic hybrid material has been compared with the standard JCPDS cards having number 38-1388. The XRD crystallite size has been calculated by using Scherrer equation Dp = 0.94λ/β$_{1/2}$Cosθ, where Dp = Average crystallite size, β = Line broadening in radians, θ = Bragg angle and λ = X-ray wave length. By Dp calculator using Scherror formula, wavelength = 1.54061Å, peak width = 0.2° and peak position = 10.911° we get the crystallite size = 42.6nm and lattice strain = 0.0081. The small peak within the range of 1000 to 2000 counts per second shows the presence of chlorine atoms and the highest peak of 9406 depicts the presence of Hg and these results are inaccordance with other hybrid materials [11]. Figure 2 depicts that the powder XRD pattern of MOF's are analogous with the XRD study of the [HgCl$_4$]$^-$ [C$_5$H$_6$ N$_2$Cl]$^+$. It shows that the inorganic component is finely crystallized with the organic moiety. The Figure 3 shows the MOF pattern of [HgCl$_4$]$^-$ [C$_5$H$_6$ N$_2$Cl]$^+$.
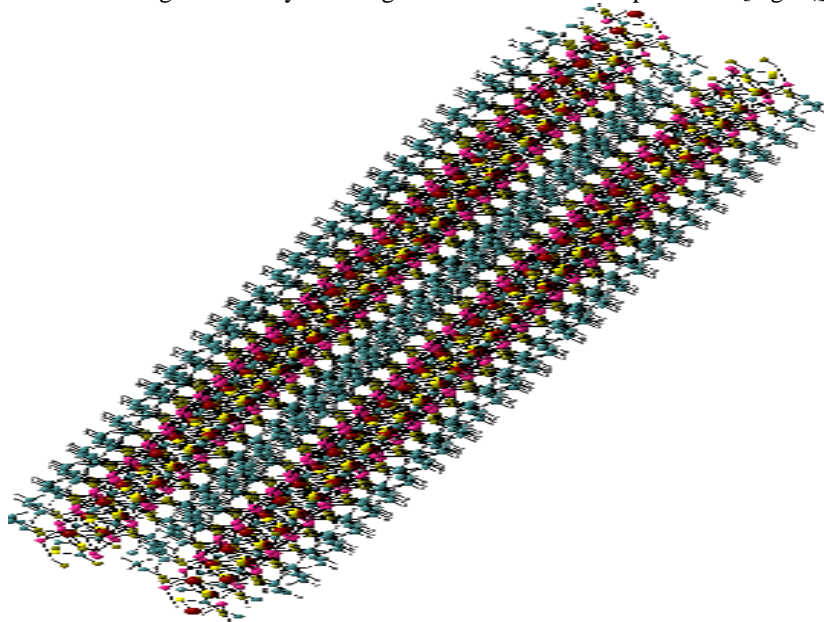
Figure 3: MOF pattern of [HgCl$_4$]$^-$ [C$_5$H$_6$ N$_2$Cl]$^+$

Field Emission scanning electron micrograph of MOF of [HgCl$_4$]$^-$ [C$_5$H$_6$ N$_2$Cl]$^+$ is presented in Figure 4. Field Emission Scanning electron microscopy is a technique that enables the study of the microstructure of nanoparticles of matter. The FESEM micrograph Figure 2 show distribution of particles in [HgCl$_4$]$^-$ [C$_5$H$_6$ N$_2$Cl]$^+$ MOF as clusters of needle shaped arranged like clusters needles. The FESEM show the crystal needles in a special arrangement forming a crystalline flower. FESEM of [HgCl$_4$]$^-$ [C$_5$H$_6$ N$_2$Cl]$^+$ MOF, show irregular flake particles. A high magnification Figure 2 right top side confirms these flakes-like particles having irregular shapes. A comparison of the FESEM micrographs of [HgCl$_4$]$^-$ [C$_5$H$_6$ N$_2$Cl]$^+$ MOF with other have crystals in a irregular arrangement unlike the flake-like particles of MOF without a regular arrangement.

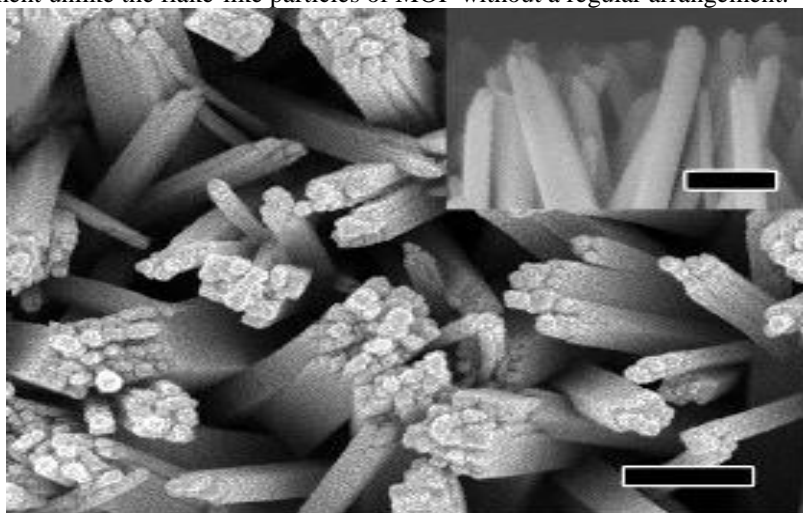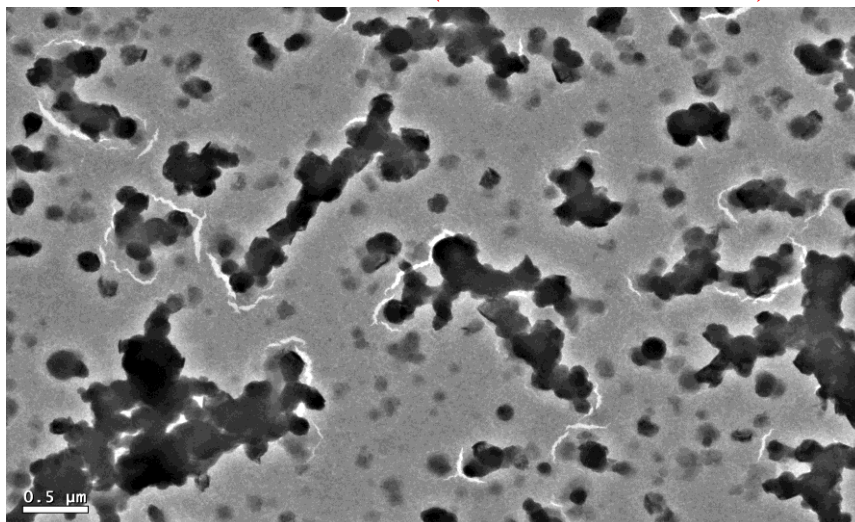Figure 4: FESEM image of MOF. Scale bars: 200 nm

Figure 5: TEM image of MOF

Transmission electron micrograph of $[HgCl_4]^-$ $[C_5H_6 N_2Cl]^+$ MOF is presented in Figures 5. The TEM micrograph for $[HgCl_4]^-$ $[C_5H_6 N_2Cl]^+$ MOF, Figure 5 at 0.5 µm respectively show a wide distribution of nanocrystals of the metal as black dots evenly distributed in the solid matrix.

Porosity of synthesized MOFs of $[HgCl_4]^-$ $[C_5H_6 N_2Cl]^+$ porphyrin paddle-wheel framework MOFs containing different dinitrogen linking ligands all exhibited thermogravimetric behavior consistent with that of porous materials, losing between 24% and 94% of their mass as solvent. As expected, the relationship between pillar size and weight percent lost during heating correlated well with $[HgCl_4]^-$ $[C_5H_6 N_2Cl]^+$ only losing 24% of its mass as solvent. $[HgCl_4]^-$ $[C_5H_6 N_2Cl]^+$ with its heterogeneous pore sizes, lost more mass as solvent then its homogenous cobalt analog.
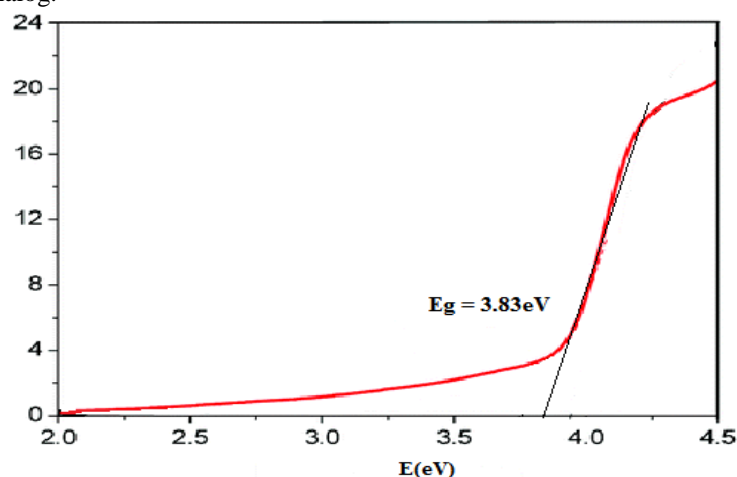

Figure 6: UV-Vis absorption spectra of MOF.

The UV-Vis spectroscopic technique was used to calculate the optical energy band gap in the hybrid materials. UV-Vis absorption spectra of $[HgCl_4]^-$ $[C_5H_6 N_2Cl]^+$ have been recorded within the wavelength range of 200 to 800 nm. The optical band gap (Eg = 3.83eV) as shown in Figure 6 and has been calculated by linear fit profile of Tauc plot for direct allowed transition. The materials having direct band gap of 3.83eV can be used in various applications such as solar cells, electronic, opto-electronic devices, organic light emitting diodes and gas sensors etc. [12, 13].

Metal-organic frameworks (MOFs) are very promising multifunctional luminescent materials because of their inherent advantages of organic linkers and inorganic metal ions as well as the tailorability in terms of structure, dimension, size and shape. Furthermore the metal centers, organic linkers, metal-organic charge transfer and guest molecules within porous MOFs all can potentially generate luminescence. Such uniqueness can allow us to generate luminescent MOF materials with systematically varied luminescence properties which are crucial for the lighting, display and optical devices. Although luminescent MOFs are still in their infancy, the currently available results have unambiguously demonstrated that the design and construction of MOFs for luminescent functionality is very active [14].

The most widely examined use for MOFs is gas storage toward alternative, clean mobile energy. Two of the main candidates being examined include hydrogen gas and methane gas. Hydrogen certainly represents the cleaner (greener) option but the difficulty of producing, safely storing, and transporting hydrogen in large

International Journal of Current Research and Modern Education (IJCRME)
Impact Factor: 6.725, ISSN (Online): 2455 - 5428
(www.rdmodernresearch.com) Volume 2, Issue 2, 2017

quantities has limited its utility to date. Hydrogen is attractive due to the high energy output with low environmental effect since water is its combustion by-product. Transport of hydrogen represents a significant challenge due to its low molecular weight and very weak attractive forces between hydrogen molecules. The storage for hydrogen in a given space at a given temperature and pressure can be increased by physisorptive binding of hydrogen to a surface, which enables closer packing of its molecules by weakly attractive forces. MOFs, as the highest surface area materials known, represent the best opportunity to meet these requirements. Separation and purification applications represent further opportunities for MOFs. Often, energy-intensive processes, such as distillation or conversion of one component into something more easily removeable, are used to achieve difficult separations. Simplifying these processes could mean significant savings of energy resources. Therefore, in the context of energy applications, the separation of CO_2 from flue gas using MOFs will be discussed in our article below.

Although initial reports of high levels of room temperature hydrogen storage in MOFs generated much interest, the failure to reproduce these initial results has led to a shift towards cryogenic storage. Cryogenic hydrogen storage has now been studied in a variety of MOFs, including MOF-177, which was shown to reversibly uptake 7.5 wt % hydrogen at 77 K (-196 °C) and ca. 55 bar. Figure 7 illustrates MOF-177's superiority over other MOFs in terms of high-pressure hydrogen storage. Although this result remains far from the DOE YR2015 goal of 7.5% for a storage system, it still represents among the highest excess hydrogen uptake for a physisorptive material. Higher surface area MOFs generally trend toward higher hydrogen storage capacity, but it cannot be assumed that a high surface area always implies higher capacity, as shown in the case of UMCM-2.[3] The BET surface area of this MOF is 5,200 m^2/g, the highest of all published materials, yet the excess gravimetric hydrogen uptake at 6.9 wt % for UMCM-2 still falls short of that for MOF-177. This could be related to pore volume, pore shape, and/or other features that have not yet been fully recognized in MOFs. Thus, there remain considerable challenges and opportunities to rationally increase hydrogen storage capacity in MOFs beyond their current levels.
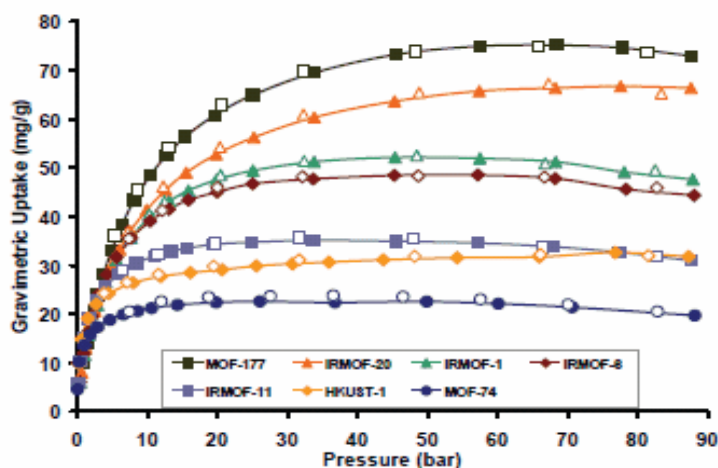

Figure 7: Hydrogen storage in different MOFs. Adsorption data are shown as closed circles, desorption data as open circles.

A large amount of research has focused on increasing the affinity of MOFs for hydrogen while maintaining high surface area and the reversibility of adsorption and desorption. To do this would entail increasing the heat of hydrogen adsorption. The factors that govern the heat of adsorption are poorly understood for physisorptive materials, but it is speculated that they may include the incorporation of small pores, pore shape (cylindrical vs. rectangular, etc.), and coordinatively unsaturated metal centers, each of which could promote tight binding of hydrogen. Until recently, MOF-505, a Cu-based MOF formed from biphenyl-3,5,3',5'-tetracarboxylic acid, has been cited as being the highest capacity, low pressure hydrogen uptake material (2.6 wt %) at 77 K and 1 atm, which indicates its high heat of hydrogen adsorption and a strong hydrogen affinity. UMCM-150, another Cu-based material, has a lower heat of adsorption for hydrogen at 7.3 kJ/mol. However, it still displays impressive excess gravimetric hydrogen uptake of 2.1 wt % at 77 K and 1 bar due to significantly higher surface area than MOF-505. MOF-74 and Co-, Ni-, and Mg-based analogs, which are all formed using 2,5-dihydroxyterephthalic acid (Aldrich Prod. No.382132), have small cylindrical pores with coordinatively unsaturated metal centers. They are also known to have high heats of adsorption for hydrogen at 77 K and 1 atm. These MOFs are generally limited by relatively low surface areas, though. Hupp and coworkers have used post-synthetic modification of a Zn-based 1,2,4,5-tetrakis(4'-carboxyphenyl) benzene (Aldrich Prod. No. 715298), 3-di(4-pyridyl)-2,3-butanediol (Aldrich Prod. No.43653) pillared MOF with lithium or magnesium ions to increase affinity and uptake of hydrogen. Unfortunately, their material demonstrated only low surface areas of (ca. 800 m^2/g). It should be noted that increasing hydrogen affinity in the low pressure regime may

International Journal of Current Research and Modern Education (IJCRME)
Impact Factor: 6.725, ISSN (Online): 2455 - 5428
(www.rdmodernresearch.com) Volume 2, Issue 2, 2017

ultimately have limited value. The operating pressure for a storage system is unlikely to be less than 1 atm, meaning that uptake below this pressure is essentially wasted on gas that can not be delivered.

Compressed natural gas (CNG) vehicles are already on the road today. Gas (methane) pressures in the fuel tank of such vehicles can approach 3,600 psi (248 bar). To reach similar economical energy output, yet improve safe storage and transport, the DOE has set targets for methane storage of 180 v(STP)/v (v(STP) = standard temperature and pressure of methane; v = volume of adsorbent) under 35 bar. A number of MOFs in the IRMOF series, i.e., Zn-based MOFs with the same metal cluster but varying linear organic linkers, were tested for methane storage. IRMOF-6 (155 cm^3(STP)/cm^3) was found to be the highest in this series surpassing MOF-5 (135 cm^3(STP)/cm^3) and IRMOF-3 (120 cm^3(STP)/cm^3) at 36 atm. Examination of the Raman spectra of the adsorbed methane at pressures of up to 30 bar in the IRMOF series revealed that variation in the organic linker alone can significantly influence the adsorption affinity of methane in these materials. Zhou has recently reported that a Cu-MOF, PCN-14, with an anthracene-based linker can demonstrate high uptake of methane (absolute methane adsorption capacity estimated to be 230 v/v at 35 bar and 290 K). Although an impressive accomplishment, some doubt has been expressed that this has in fact exceeded the DOE target, based, in part, on the difference between a crystallographic density and a bulk packing density.

Even with the global push for alternative energy, carbon dioxide emission remains a growing concern. For example, if methane gas were implemented as a primary fuel source, CO_2 would still be emitted as a by-product of combustion. Currently the largest single point sources of CO_2 emission are power plants that produce streams of flue gas, exhausted combustion smoke, with CO_2 concentrations of ca. 15% at 1 atm.
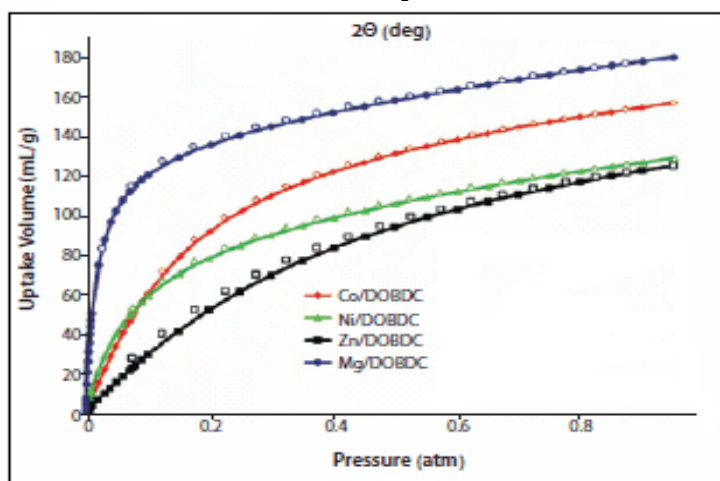

Figure 8: Low-pressure carbon dioxide adsorption for analogs of MOF-74 (Co[II], Ni[II], Mg[II], and Zn[II]).

While storage of CO_2 is not much of a challenge, the separation of CO_2 from streams of flue gas represents a significant problem that must be addressed by the development of high CO_2 affinity materials before any thought of geologic sequestration can be effectively implemented. We recently published data on the use of MOF-74, a Zn-based material, and its Co-, Ni-, and Mg-based analogs in the uptake of CO_2 at low pressure. The Mg-based analog of MOF-74 (Mg/DOBDC) was found to uptake ca. 35 wt % CO_2 at 1 atm and RT Figure 8. This value is significantly higher than that of any other physisorptive material under the same conditions including zeolite 13X (molecular sieve type 13X). Since our report, Blom, Dietzel, and co-workers have confirmed our results and reported an X-ray crystal structure data showing CO2 molecules bound to the metal centers in the Ni-based analog of MOF-74. Accomplishing such uptakes in the presence of other components in flue gas is ultimately needed to contemplate replacing existing capture technologies based on chemisorption by amines.

4. Conclusion:

The active electro-optical devices are the key components in current and future data transfer technologies and in order to fulfill future requirements in miniaturization for diffractive, refractive and integrated optical devices, the inorganic-organic hybrid derivatives produced at fairly low costs with a high degree of reproducibility are now proven materials. The bis[2-amino-5-chloropyridine tetrachlorozincate(II)], a MOF derivative depicts the role of hydrogen bonds in holding the inorganic and organic moieties into a single composite. The powder XRD predicts that such materials can be used as electro-optical sensors with high sensitivity.

Metal-organic frameworks, a subset of coordination polymers, represent a powerful new tool for a plethora of alternative energy applications. MOFs are readily available using simple synthetic strategies that supply tailored, high surface area materials. Current MOF technology sets the standard for cryogenic and room temperature storage of hydrogen and methane, respectively. Furthermore, new opportunities in separations using MOFs provide the prospect of clean, alternative energy capabilities.

Acknowledgement:

References:

1. Cui, Y. Bin, L. Huajun, H. Wei, Z. Banglin, C. & Guodong Q. 2016. Metal–organic frameworks as platforms for functional materials. Acc. Chem. Res 49(3), 483-493.
2. Alawisi, H. Li, B. He, Y. Arman, H. D. Asiri, A. M. Wang, H. & Chen, B. (2014). A microporous metal–organic framework constructed from a new tetracarboxylic acid for selective gas separation. Crystal Growth & Design, 14(5), 2522-2526.
3. Della, R. J. Liu, D. & Lin, W. (2011). Nanoscale metal–organic frameworks for biomedical imaging and drug delivery. Accounts of chemical research, 44(10), 957-968.
4. Islamoglu, T. Goswami, S. Li, Z. Howarth, A. J. Farha, O. K. & Hupp, J. T. (2017). Postsynthetic Tuning of Metal–Organic Frameworks for Targeted Applications. Accounts of Chemical Research, 50(4), 805-813.
5. Tian, Z. Dai, S. & Jiang, D. E. (2016). Site partition: turning one site into two for adsorbing CO2. The journal of physical chemistry letters, 7(13), 2568-2572.
6. Stavila, V. Talin, A. A. & Allendorf, M. D. (2014). MOF-based electronic and opto-electronic devices. Chemical Society Reviews, 43(16), 5994-6010.
7. Stavila, V. Talin, A. A. & Allendorf, M. D. (2014). MOF-based electronic and opto-electronic devices. Chemical Society Reviews, 43(16), 5994-6010.
8. Hendon, C. H. Wittering, K. E. Chen, T. H. Kaveevivitchai, W. Popov, I. Butler, K. T. & Walsh, A. (2015). Absorbate-induced piezochromism in a porous molecular crystal. Nano letters, 15(3), 2149-2154.
9. Roisnel, T. Carvajal, J. R. (2000). EPDIC.
10. Rodriguez, C. J. (1993). Recent advances in magnetic structure determination by neutron powder diffraction. Physica B: Condensed Matter, 192(1-2), 55-69.
11. Kawazoe, S. Sakamoto, K. Awamura, Y. Maruyama, T. Suzuki, T. Onda, K. & Takasu, T. (2008). Beta-form crystal of acetanilide derivative, EP1932838A2 (European Patent).
12. Schulz, M. J. Kelkar, A. D. & Sundaresan, M. J.2005. Nano engine. of struct. Funct. and smart mat. Taylor & Francis, 20.
13. Bourguiba, F. Dhahri, A. Tahri, T. Taibi, K. Dhabri, J. & Hill, E. k. 2016. Bull. Mat. Sci. 39, 1765.
14. Cui Y., Chen B., Qian G. (2013) Luminescent Properties and Applications of Metal-Organic Frameworks. In: Chen B., Qian G. (eds) Metal-Organic.

.